

## ON THE ORIGIN OF THE TAILWARD VELOCITY OF O<sup>+</sup> IONS OVER THE MAGNETIC POLES OF MARS

M. Reyes-Ruiz,<sup>1</sup> H. Aceves,<sup>1</sup> and H. Pérez-de-Tejada<sup>2</sup>

Received 2009 August 17; accepted 2010 January 11

### RESUMEN

A partir del análisis de la dinámica de iones O<sup>+</sup> de origen ionosférico en la ionofunda de Marte, acelerados por el campo eléctrico convectivo del viento solar (*pick up ions*), determinamos su velocidad promedio sobre los polos magnéticos del planeta. Estas velocidades se comparan con mediciones *in situ* de la nave Mars Express. Con base en nuestros resultados encontramos que las velocidades de los iones O<sup>+</sup> medidos sobre los polos magnéticos del planeta, que son esencialmente en la dirección antisolar, con componentes *y* y *z* muy pequeñas, no se pueden explicar en términos del movimiento girotrópico de las partículas exclusivamente. Concluimos entonces que la velocidad de los iones O<sup>+</sup> sobre los polos magnéticos del planeta resultan de la acción de fuerzas de tipo viscoso que transfieren momento entre el viento solar y el plasma ionosférico en la ionofunda de Marte.

### ABSTRACT

We numerically simulate the dynamics of a population of O<sup>+</sup> ions of ionospheric origin picked-up by the solar wind in the dayside ionosheath of Mars. Their average velocity as they reach the magnetic polar regions of the planet is compared with *in situ* measurements of the Mars Express spacecraft. We find that the velocity of O<sup>+</sup> ions measured over the magnetic poles of the planet, which is essentially tailward with very small *y* and *z*-components according to measurements, cannot be accounted for solely in terms of particle gyromotions. We suggest that the velocity of O<sup>+</sup> ions over the magnetic poles of the planet is more probably the result of wave-particle interactions that mediate the transfer of momentum from the solar wind plasma to ionospheric plasma and newly born ions in the ionosheath.

*Key Words:* planets and satellites: individual (Mars) — plasmas — solar wind

### 1. INTRODUCTION

The *in situ* measurements obtained with the Analyser of Space Plasmas and Energetic Atoms (ASPERA-3) instrument on board the Mars Express spacecraft (Barabash et al. 2006) have yielded results of great importance for our understanding of the interaction of the solar wind with ionospheric plasma over the magnetic polar regions of Mars and other non-magnetic bodies in the solar system (e.g., Lundin et al. 2008). Among these results, it has been found that, at least occasionally, the velocity of ionospheric O<sup>+</sup> ions in the ionosheath over the magnetic poles of the planet is contained essentially

in the antisunward (*x*) direction (Pérez-de-Tejada et al. 2009). It is difficult to ascertain how frequently this condition occurs, since velocity data for O<sup>+</sup> ions are not yet available in the literature.

Pérez-de-Tejada et al. (2009) have argued that the observation described above is not easily explained solely in terms of the standard picture of  $\mathbf{E} \times \mathbf{B}$  drift of picked-up O<sup>+</sup> ions in the ionosheath (e.g., Luhmann & Schwingenshuh 1990, and references therein) for the following reasons: on one hand, the gyromotion of newly born ions in the vicinity of the magnetic poles is expected to occur essentially in the vertical direction (*z*), with a much smaller tailward (*x*) component, precisely the opposite to the measurements of Mars Express. Also, the velocity of O<sup>+</sup> ions, as they  $\mathbf{E} \times \mathbf{B}$  drift in the convective electric field set up by the streaming solar wind, is expected

<sup>1</sup>Instituto de Astronomía, Universidad Nacional Autónoma de México, Ensenada, B. C., Mexico.

<sup>2</sup>Instituto de Geofísica, Universidad Nacional Autónoma de México, Mexico.

to reach a maximum velocity that is greater (by up to a factor of 2) than the solar wind velocity in the region; again in contradiction with *in situ* measurements. This has led Pérez-de-Tejada et al. (2009) to conclude that the  $O^+$  velocities in the magnetic polar regions of these planets are not the result of  $\mathbf{E} \times \mathbf{B}$  drift, but instead acquire their velocity mainly from the viscous-like transfer of solar wind momentum to ionospheric plasma.

It is worth recalling that the action of viscous-like forces in the ionosheath of Mars over the magnetic polar regions, and in other nonmagnetic solar system bodies such as Venus and comets, has been shown to be a natural explanation to several other properties of the flow as measured by spacecraft since the Mariner 5 flyby (Pérez-de-Tejada & Dryer 1976). Briefly, both Phobos 2 and ASPERA-3 measurements have revealed the existence of a velocity boundary layer over the magnetic polar regions and in the Mars near wake (e.g., Lundin et al. 1990; Lundin et al. 2004). This feature is similar to that observed in the ionosheath of Venus over and downstream from the magnetic poles of the planet. A velocity boundary layer has been measured in Venus by the Mariner 5 spacecraft (Bridge et al. 1967; Shefer, Lazarus, & Bridge 1979), by the Venera 10 spacecraft (Romanov, Smirnov, & Vaisberg 1979), by the Pioneer Venus Orbiter (Pérez-de-Tejada, Intriligator, & Scarf 1985) and more recently by the Venus Express spacecraft (Pérez-de-Tejada & Lundin 2008).

The ionosheath feature described above has been identified as a “viscous” boundary layer associated with the transfer of solar wind momentum to ionospheric plasma. Simultaneous with the velocity decrease measured by Mariner 5 and Venera 10, there is an increase in plasma temperature and a decrease in the density of the solar wind plasma, that clearly suggests the viscous-like nature of this boundary layer (Pérez-de-Tejada et al. 1985). As discussed by Pérez-de-Tejada (2001, 2004), in Venus this feature is related to the erosion of the upper ionosphere and to the formation of ionospheric channels that extend downstream from the magnetic poles and into the near wake. In Mars, the velocity boundary layer has also been related to the erosion of the planetary ionosphere by Pérez-de-Tejada (1998) and more recently by Pérez-de-Tejada et al. (2009). For a review of the observations and processes associated with viscous-like boundary layers in Venus and Mars the reader is referred to Pérez-de-Tejada (1995). References to more recent work can be found in Reyes-Ruiz, Díaz-Méndez, & Pérez-de Tejada (2008) and Pérez-de-Tejada et al. (2009).

The precise origin of the viscous-like processes responsible for the dynamical coupling of solar wind and ionospheric plasma is not yet determined. Attempts to determine the value of the transport coefficients in order for viscous flow models to be consistent with *in situ* measurements of the solar wind flow in the ionosheath yield a value of the effective Reynolds number (the ratio of the characteristic viscous timescale to the crossing timescale for a given flow) of approximately 20 (Pérez-de-Tejada 2005; Reyes-Ruiz et al. 2008, and references therein). Since this value is much smaller (corresponding to a higher viscosity coefficient) than that predicted from the “molecular” viscosity coefficient of the plasma in the ionosheath (Pérez-de-Tejada 2005), we refer to it as an effective or anomalous Reynolds number. A clue as to the origin of this increased efficiency of the momentum transport processes lies in the observation that the magnetic field in the ionosheath of Mars, as well as Venus and comets, has been measured to be strongly fluctuating, presumably turbulent, by numerous spacecraft (e.g., Riedler et al. 1991; Acuña et al. 1998; Bertucci et al. 2004). As is well known in fluid dynamics, turbulence usually increases the transport coefficients, viscosity included, by orders of magnitude over the “molecular” values (Lesieur 1991).

The purpose of this work is to demonstrate in a quantitative manner that simple gyromotion of newly born ions in the magnetic polar regions of Mars does not lead to average velocities similar to those measured by the Mars Express spacecraft; i.e., mainly in the  $x$ -direction (tailward). To do this we compute the trajectory of picked-up ions in a magnetic field and solar wind velocity model applicable to the dayside ionosheath of Mars. The methodology to compute the dynamics and calculate the average velocities, as well as the magnetic field and solar wind velocity models, is described in § 2. A brief description of the *in situ* measurements of the Mars Express spacecraft used in this study is given in § 3, and results are presented in § 4. In § 5 we compare these results to *in situ* measurements of  $O^+$  ions velocities in Mars and discuss a possible alternative explanation for the measured velocity behavior. We present our concluding remarks in § 6.

## 2. MODEL DESCRIPTION AND METHODOLOGY

In this section we describe the numerical methods used to compute the trajectory of newly born  $O^+$  ions in the ionosheath of Mars. We also describe the calculation of average velocities and the mag-

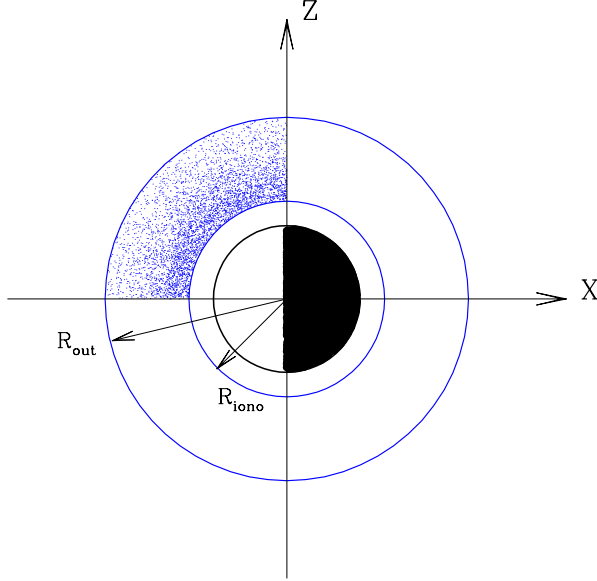


Fig. 1. Illustration of the geometry of the problem and a typical initial distribution of particles.

netic field and solar wind velocity models used for the dayside ionosheath of the planet.

### 2.1. Particle Dynamics

We solve the equation of motion of newborn ions in 2D, assuming that the majority of ions reaching the magnetic poles move approximately in the  $xz$  plane and that the magnetic field in this noon-midnight plane is always in the  $-y$  direction (see Figure 1). For a particle of mass  $m$  and electric charge  $q$ , newly born in a medium with magnetic field  $\mathbf{B} = [0, -B_o(x, z), 0]$  and a streaming solar wind with velocity contained in the  $xz$  plane,  $\mathbf{U} = [U_x(x, z), 0, U_z(x, z)]$ , the non-relativistic Lorentz equation of motion, split into components, can be written as:

$$\frac{dV_x}{dt} = -\Omega U_z + \Omega V_z, \quad (1)$$

and

$$\frac{dV_z}{dt} = \Omega U_x - \Omega V_x, \quad (2)$$

where  $V_x$  and  $V_z$  are the  $x$  and  $z$  component of the velocity of the particle,  $\Omega = qB_o/mc$  is the gyrofrequency, a function of  $x$  and  $z$  in general, and  $c$  is the speed of light. Since we are interested in O<sup>+</sup> ions we use  $m = 16m_H$  and  $q = e$  in our calculations. The equation of motion for the  $y$ -component is decoupled from the  $x$  and  $z$  equation and is not considered in this 2D study.

This system of equations is solved numerically using a 4th-order Runge-Kutta scheme. The timestep used is 0.01 of the minimum value of the gyroperiod in our model (approximately), i.e. that corresponding to the maximum  $|B|$  and minimum  $U$ . We have run several cases with a timestep up to 2 orders of magnitude smaller with no noticeable differences in our results, so we may safely conclude that the numerical solution has achieved convergence.

The origin of the coordinate system used in these calculations is located at the center of the planet. Particles are injected simultaneously in a region extending from the top of the ionosphere (located at  $R_{\text{iono}}$ ) to an outer radius  $R_{\text{out}}$ . Particles are initially distributed in a random manner weighted by a density distribution taken to mimic a spherically symmetric, exponentially decreasing density (with radius) of a neutral exosphere, from which the newly born ions are formed. As an example, a realization of the initial distribution of 1000 particles is shown in Figure 1, where the geometry of the problem is also illustrated. The dayside ionosheath region, where the O<sup>+</sup> ions are born, is assumed to extend from the ionopause (at  $R_{\text{iono}}$ ) located at an altitude of 600 km, to the bow shock, assumed to be located at a radius  $R_{\text{out}} = 1.65 R_M$ , where  $R_M$  is the Martian radius. This geometry is adopted for simplicity. We have decreased the values of  $R_{\text{iono}}$  and increased  $R_{\text{out}}$  by a factor of 2 and found no differences that could significantly affect our conclusions.

All particles are assumed to start from rest, *i.e.*  $V_x(t=0) = V_z(t=0) = 0$  for all particles; consistent with the very low thermal velocity of newly born O<sup>+</sup> ions as compared to the streaming solar wind velocity in the region ( $|\mathbf{U}|$ ).

The dynamics of a large collection of particles,  $N = 10^4$ , is followed until they reach the terminator or collide with the ionosphere of the planet (at  $r = R_{\text{iono}}$ ). The O<sup>+</sup> ions reach the terminator at different heights depending on their initial position and on the properties of the magnetic field and solar wind flow in the dayside ionosheath of the planet.

We have chosen to calculate the average velocity of the O<sup>+</sup> ions at different heights as they cross the terminator. We consider these locations as representative of the region where the Mars Express spacecraft conducted measurements (see § 3) in the vicinity of the magnetic poles.

To calculate the average velocity of O<sup>+</sup> ions over the magnetic poles we bin the particles into  $n_{\text{bin}} = 50$  intervals in the  $z$  coordinate (altitude over the magnetic pole), and simply sum the velocity of all particles passing over the pole in a given bin to cal-

culate their average velocity. Since only ions coming from the daytime northern/southern hemisphere reach the northern/southern magnetic pole, we focus on the quadrant corresponding to  $-x, +z$  coordinates in Figure 1.

### 2.2. Dayside ionosheath models

The vertical profiles of  $V_x$  and  $V_z$  of the  $O^+$  ions over the magnetic poles, depend on the configuration of the magnetic field, and the solar wind flow model for the daytime ionosheath. For each of these quantities we adopt a model that resembles their variation with solar zenith angle ( $SZA = \theta$ ) going from the subsolar point to the magnetic poles of the planet, as found in the gasdynamic models of Spreiter & Stahara (1980). The precise models we use to compute the trajectory of the ions have the following properties:

1. The magnetic field decreases “sinusoidally” from a maximum intensity ( $B_{\max}$ ) at the subsolar point to a minimum intensity at the magnetic poles ( $B_{\min}$ ) according to:

$$B_o(x, z) = (B_{\max} - B_{\min}) \cos \theta + B_{\min}, \quad (3)$$

where  $\theta = \tan^{-1}|z/x|$ .

2. The speed of the solar wind in the dayside ionosheath is assumed to be always tangential to the ionopause and to increase sinusoidally from a minimum velocity at the subsolar point,  $U_{\min}$ , to a maximum velocity at the magnetic poles,  $U_{\max}$ , according to:

$$|\mathbf{U}(x, z)| = (U_{\max} - U_{\min}) \sin \theta + U_{\min}, \quad (4)$$

$$U_x(x, z) = -|\mathbf{U}(x, z)| \sin \theta, \quad (5)$$

and

$$U_z(x, z) = |\mathbf{U}(x, z)| \cos \theta, \quad (6)$$

where  $\theta$  is the angle from the  $-x$ -axis.

The precise values of  $B_{\max}$ ,  $B_{\min}$ ,  $U_{\max}$  and  $U_{\min}$  determine the vertical velocity profile for the picked-up  $O^+$  ions over the magnetic poles.

### 3. IN SITU MEASUREMENTS

The ASPERA-3 instrument on board the Mars Express spacecraft measured the properties of both the solar wind and the ionospheric  $O^+$  flow over the magnetic poles of the planet. For example, during orbit 4032 (corresponding to February 25, 2007), shortly after periapsis, the spacecraft flew over the

polar regions of the planet which, as has been argued by Pérez-de-Tejada et al. (2009), more or less coincide with the magnetic poles. Between 17:10 and 17:20 hours the spacecraft went from an altitude of approximately 700 km over the surface of the planet to almost 2000 km. During this portion of its orbit the spacecraft remained slightly on the nightside of the terminator and within  $10^\circ$  of the poles of the planet. Pérez-de-Tejada et al. (2009) have argued that during this time the spacecraft moved through a boundary layer resulting from the direct, viscous-like interaction of the solar wind and ionospheric plasma.

An interesting property of the bulk velocity of  $O^+$  ions in the polar region is that it is greatly dominated by the  $x$  component. The ratios  $V_x/V_y$  and  $V_x/V_z$  are always greater than 5 and typically around 10. Also, over this region the essentially tailward velocity of the  $O^+$  ions reaches, at most,  $200 \text{ km s}^{-1}$ , while the speed of the solar wind  $H^+$  ions is approximately  $250 \text{ km s}^{-1}$  (Pérez-de-Tejada et al. 2009). Qualitatively similar results are found in the measurements of Venus Express over the magnetic polar regions of Venus (Pérez-de-Tejada & Lundin 2008).

## 4. RESULTS

We present results for a series of cases with different values of the dayside ionosheath magnetic field configuration,  $B_{\max}$ ,  $B_{\min}$ , and of the solar wind flow properties,  $U_{\max}$  and  $U_{\min}$ .

In the models of Spreiter & Stahara (1980) the magnitude of the  $y$  component of the draped interplanetary magnetic field (IMF) at the subsolar point of a non-magnetic planet, such as Venus or Mars, is approximately 6–8 times the magnitude of the pre-shock IMF. According to Acuña et al. (1998), measurements from the Mars Global Surveyor (MGS) mission indicate that the pre-shock magnetic field is typically around 5 nT. This implies a magnetic field intensity at the subsolar point,  $B_{\max}$ , ranging from 30 to 60 nT approximately. As pointed out by Crider et al. (2004) the MGS measured magnetic field intensities in the dayside ionosheath are in good agreement with the gasdynamics calculations of Spreiter & Stahara (1980). The measurements of MGS also indicate that the magnetic field intensity in the ionosheath over the magnetic poles of the planet is approximately 2–3 times the value of the preshock IMF (Crider et al. 2004). Hence, in our model we adopt a value of  $B_{\min}$  ranging from 10 to 20 nT.

We also follow Spreiter & Stahara (1980) in setting the value of the velocity of the shocked solar wind, as it flows from the subsolar point to the mag-

TABLE 1  
DESCRIPTION OF THE MODEL  
PARAMETERS USED IN EACH OF THE CASES  
PRESENTED

Case	$B_{\max}$	$B_{\min}$	$U_{\max}$
1	60	10	250
2	60	20	250
3	30	10	250
4	30	20	250
5	45	20	200
6	45	20	300

netic poles of the planet. At the subsolar point we adopt a very low flow velocity,  $U_{\min} = 0.01 V_{\text{SW}}$ , where  $V_{\text{SW}}$  is the speed of the pre-shock solar wind at Mars. In the models of Spreiter & Stahara (1980) the solar wind velocity over the magnetic poles is approximately  $0.75 V_{\text{SW}}$ . Using the typical value  $V_{\text{SW}} = 350 \text{ km s}^{-1}$  (consistent with the ASPERA-3 measurements) we adopt  $U_{\min} = 3 \text{ km s}^{-1}$  and  $U_{\max} = 250 \text{ km s}^{-1}$ . To explore the effect of a variation in  $V_{\text{SW}}$  we also present the results for two models with  $U_{\max} = 300$  and  $U_{\max} = 200 \text{ km s}^{-1}$ .

Particle trajectories and average velocities have been computed for a series of cases corresponding to different model parameters ( $B_{\min}$ ,  $B_{\max}$ ,  $U_{\max}$ ) as described in Table 1. These cases are chosen to represent the expected range of values for each parameter given the uncertainty in our models of the magnetic field and flow conditions in the ionosheath, as well as the variability associated with the solar wind conditions.

#### 4.1. High $B_{\max}$ cases

Cases 1 and 2 presented in this subsection are characterized by a high value of the magnetic field strength at the subsolar point,  $B_{\max} = 60 \text{ nT}$ . This is an extreme value, corresponding to a factor of 12 compression of the pre-shock IMF.

In Figure 2 we show the trajectories for a random sample of 100 particles (of a total of 10 000 followed) to serve as an illustration of the path followed by newly born O<sup>+</sup> ions in the ionosheath of Mars. This figure corresponds to Case 1, characterized by model parameters  $B_{\min} = 10 \text{ nT}$ ,  $B_{\max} = 60 \text{ nT}$  and  $U_{\max} = 250 \text{ km s}^{-1}$ . A figure corresponding to Case 2, which has the same  $B_{\max} = 60 \text{ nT}$  and  $U_{\max} = 250 \text{ km s}^{-1}$  as Case 1, but a higher magnetic field at the magnetic poles of the planet,  $B_{\min} = 20 \text{ nT}$ , is very similar and, in the interest of brevity, is omitted.

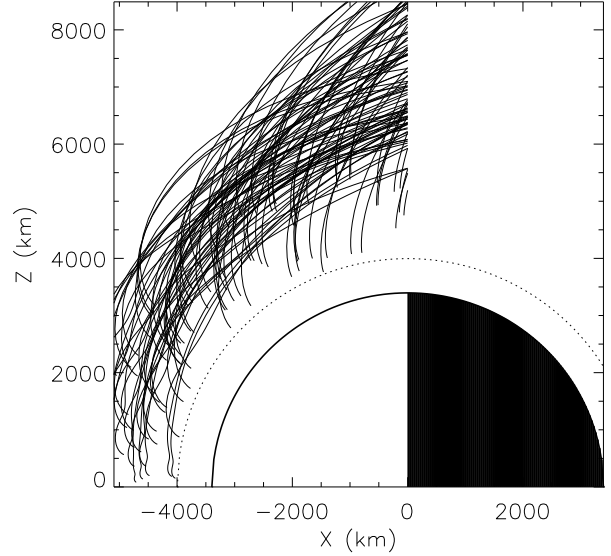


Fig. 2. Trajectory of a sample of one hundred O<sup>+</sup> ions newly born in an ionosheath characterized by  $B_{\min} = 10 \text{ nT}$ ,  $B_{\max} = 60 \text{ nT}$  and  $U_{\max} = 250 \text{ km s}^{-1}$ . The thick solid line and the dotted line represent, respectively, the surface of the planet and the assumed ionopause location in our model.

In Figure 3 we show the average velocity components,  $\langle V_x \rangle$  and  $\langle V_z \rangle$ , of the picked-up O<sup>+</sup> ions as they pass directly over the magnetic poles of the planet with an ionosheath model corresponding to Cases 1 and 2 (see Table 1). We have termed these models the high magnetic field cases, since the piled-up magnetic field at the subsolar point is somewhat stronger than that predicted by the gas-dynamic models of Spreiter & Stahara (1980). We present it as an extreme case in order to illustrate the tendency in varying this parameter,  $B_{\max}$ , as we compare it to other cases.

The top panel of Figure 3 corresponds to Case 1, characterized by  $B_{\max} = 60 \text{ nT}$ ,  $B_{\min} = 10 \text{ nT}$  and  $U_{\max} = 250 \text{ km s}^{-1}$ . At an altitude of approximately 600 km ( $R = 1.18 R_M$  in Mars-centric coordinates) where the ionopause is located in our model, both components of velocity start increasing, although  $V_z$  increases much more than  $V_x$ . At low altitudes over the magnetic poles, and up to a distance of 5400 km ( $1.58 R_M$ ) from the center of the planet,  $V_z$  is much greater than  $V_x$ , typically by a factor of 3 to 6. The essentially vertical character of the velocity of the O<sup>+</sup> is also evident from Figure 2. Upwards of 5400 km,  $V_x$  increases sharply and becomes greater than  $V_z$  by a factor of 2–3 approximately. While the velocity of ions born in the vicinity of the magnetic poles is still mainly vertical up to great heights, the *average*

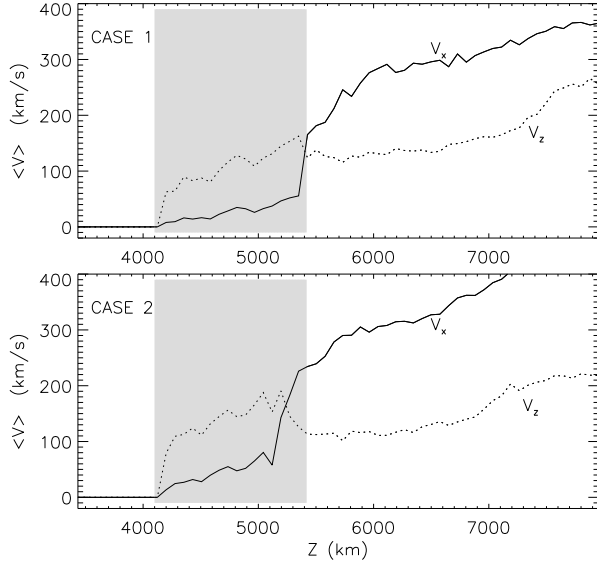


Fig. 3. Vertical profiles of the average velocity of picked-up  $O^+$  ions over the magnetic poles of the planet. The top panel corresponds to a dayside ionosheath model considered in Case 1 (see Table 1). The bottom panel corresponds to a model with the parameters of Case 2. In both figures the thick solid line shows the average value of the  $x$  component of the velocity,  $\langle V_x \rangle$ , and the dotted line shows the  $z$  component,  $\langle V_z \rangle$ . The shaded region represents the height range travelled by the Mars Express spacecraft over the magnetic poles.

velocity is contained mostly in the  $x$  direction above 5500 km, owing to the contribution of ions coming from the dayside ionosheath.

The bottom panel of Figure 3 corresponds to Case 2, in which the dayside ionosheath is characterized by the same  $B_{\max} = 60$  nT and  $U_{\max} = 250$  km s $^{-1}$  as in Case 1, but with a magnetic field at the magnetic poles that is twice as strong,  $B_{\min} = 20$  nT. The  $z$  component of the average velocity of  $O^+$  ions greatly dominates over the  $x$  component, by a factor of 2–4 approximately, up to 5250 km ( $1.54 R_M$ ) from the center of the planet. At greater heights over the magnetic poles of the planet, the average velocity of  $O^+$  ions, in this scenario, quickly exceeds 300 km s $^{-1}$  and is essentially contained in the  $x$ -direction; with  $V_x$  exceeding  $V_z$  by a factor of 3 or more.

#### 4.2. Low $B_{\max}$ cases

To assess the effect of changing the intensity of the magnetic field at the subsolar point, we present Cases 3 and 4 characterized by the same values of  $B_{\min}$  and  $U_{\max}$  as Cases 1 and 2 (respectively) but with a smaller value of  $B_{\max} = 30$  nT. This is the lowest value of  $B_{\max}$  within the expected range as

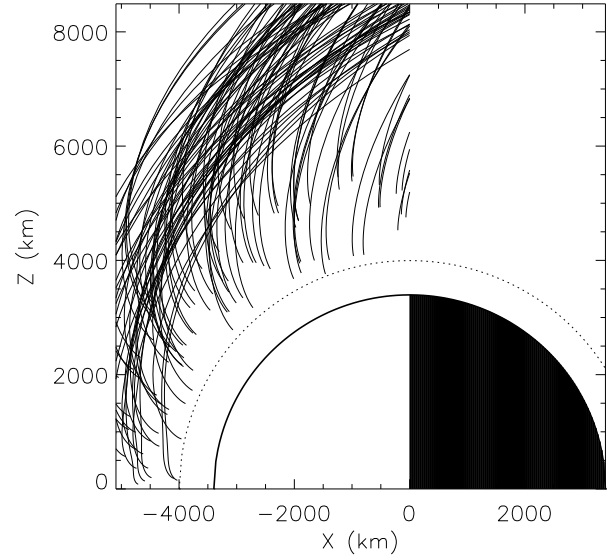


Fig. 4. Same as Figure 2 but for an ionosheath model characterized by  $B_{\min} = 10$  nT,  $B_{\max} = 30$  nT and  $U_{\max} = 250$  km s $^{-1}$ , Case 3.

discussed above, corresponding to a factor of 6 compression of the typical pre-shock IMF.

Figure 4 illustrates the typical trajectories of picked-up  $O^+$  ions in the dayside ionosheath of Mars for a model characterized by  $B_{\min} = 10$  nT,  $B_{\max} = 30$  nT and  $U_{\max} = 250$  km s $^{-1}$  (Case 3). In comparing with Figure 2, corresponding to Case 1, which has the same  $B_{\min}$  and  $U_{\max}$  km s $^{-1}$  but a higher magnetic field at the subsolar point, we see that particle trajectories are such that  $O^+$  ions born in the dayside ionosheath reach the magnetic poles of the planet at greater height and with a greater  $V_z$ . The corresponding figure showing the particle trajectories for Case 4, with a higher magnetic field at the magnetic poles (not shown) is very similar. The same effect is also seen in Figure 5 which shows the average velocity,  $\langle V_x \rangle$  and  $\langle V_z \rangle$ , of the picked-up  $O^+$  ions as they pass directly over the magnetic poles of the planet, with an ionosheath model corresponding to Cases 3 and 4 (see Table 1). The lower subsolar magnetic field in these Cases, in comparison to Cases 1 and 2, leads to a smaller value of the average  $V_x$  over the magnetic poles of the planet.

The average velocity in Case 3, shown in the top panel of Figure 5, is dominated by the vertical component,  $V_z$ , up to much greater heights than in Case 1. The horizontal velocity,  $V_x$ , increases from zero at the top of the ionosphere to 150 km s $^{-1}$  at 7500 km ( $2.2 R_M$ ) from the center of the planet, being smaller than the vertical component,  $V_z$ , by a factor

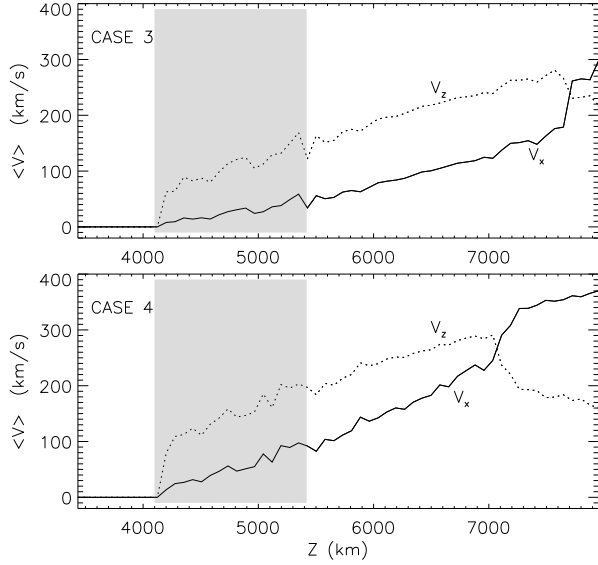


Fig. 5. Same as Figure 3 but for a dayside ionosheath model corresponding to Cases 3 (top panel) and 4 (bottom panel) as described in Table 1.

of 2–3. A comparison of Case 4 ( $B_{\max} = 30$  nT) shown in the bottom panel of Figure 5, and Case 2 ( $B_{\max} = 60$  nT) shown in Figure 3, shows the same tendency, namely, that a decrease in the magnetic field strength at the subsolar point leads to the  $z$  component of the average velocity of O<sup>+</sup> ions being dominant over a wider range of altitudes over the magnetic poles of the planet.

#### 4.3. Variation of $U_{\max}$

In Figures 6 and 7 we illustrate the effect of changing the velocity of the solar wind as it flows over the magnetic poles of the planet  $U_{\max}$ . For Cases 5 and 6 we use the same magnetic field model,  $B_{\max} = 45$  nT and  $B_{\min} = 20$  nT, but different values of  $U_{\max}$ . Case 6, for which particle trajectories are illustrated in Figure 6 and average velocity is shown in Figure 7 (bottom panel), is characterized by  $U_{\max} = 300$  km s<sup>-1</sup>. The average velocity of O<sup>+</sup> ions for Case 5, with  $U_{\max} = 200$  km s<sup>-1</sup>, is shown in the top panel of Figure 7.

As shown in Figure 6, an increase in  $U_{\max}$  also leads to more vertical particle trajectories over the magnetic poles in comparison to models with a smaller value of this parameter, e.g., Case 1 shown in Figure 2. This tendency is evident in Figure 7, where Case 5 with  $U_{\max} = 200$  km s<sup>-1</sup>, and Case 6,  $U_{\max} = 300$  km s<sup>-1</sup>, are directly compared. The vertical range over which the  $z$  component of the velocity dominates is much greater for the case with high

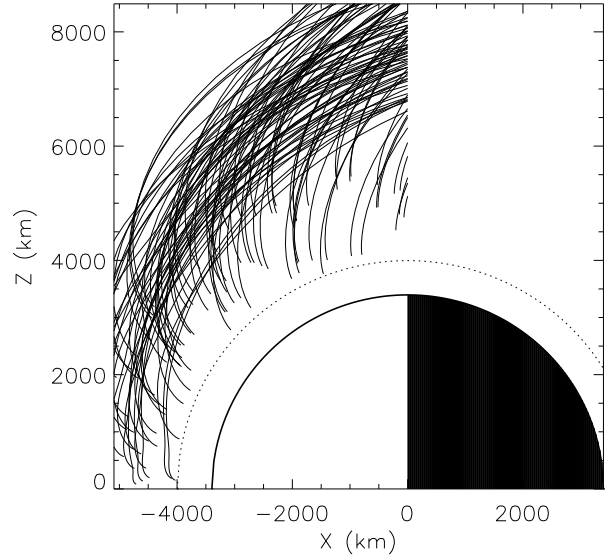


Fig. 6. Same as Figure 2 but for an ionosheath model characterized by  $B_{\min} = 20$  nT,  $B_{\max} = 45$  nT and  $U_{\max} = 300$  km s<sup>-1</sup>, Case 6.

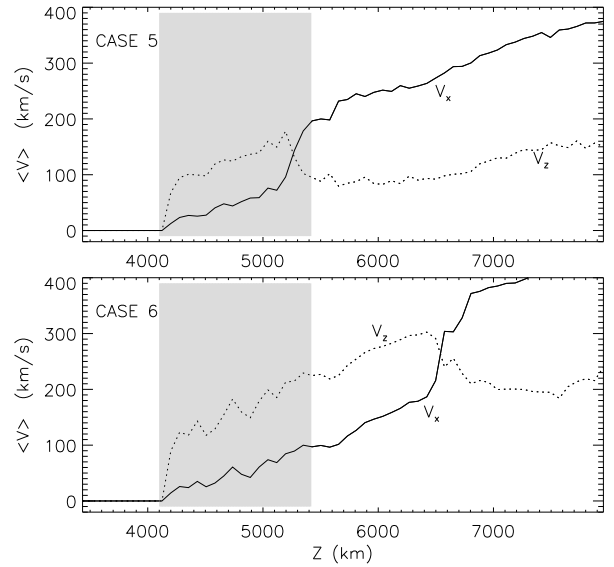


Fig. 7. Same as Figure 3 but for a dayside ionosheath model corresponding to Cases 5 (top panel) and 6 (bottom panel) as described in Table 1.

solar wind velocity over the magnetic poles (Case 6) in comparison to Case 5 (low  $U_{\max}$ ). In the case with a lower  $U_{\max}$ , the horizontal component of the velocity becomes dominant at a distance of approximately 5200 km ( $1.53 R_M$ ) from the center of the planet. Above this height, the average velocity of O<sup>+</sup> ions is greatly dominated by the horizontal ( $x$ )

component, which exceeds  $200 \text{ km s}^{-1}$ . In contrast, in the high  $U_{\text{max}}$  case, the velocity is essentially vertical;  $V_z$  is 2–3 times greater than  $V_x$ , up to about  $6500 \text{ km}$  ( $1.91 R_M$ ) from the center of the planet.

## 5. DISCUSSION

The main result of this study, evident in Figures 2 through 7, is that in the altitude range between  $700$  and  $2000 \text{ km}$  sampled by the Mars Express spacecraft over the magnetic poles of the planet, the average velocity resulting from the  $\mathbf{E} \times \mathbf{B}$  drift of  $\text{O}^+$  ions born in the dayside ionosheath of the planet, is strongly dominated by the vertical ( $z$ ) component. This result is a direct consequence of the large gyroradius that characterizes the  $\mathbf{E} \times \mathbf{B}$  drift under the magnetic field and solar wind velocity conditions expected in the dayside ionosheath of the planet.

The tendencies observed as one varies the magnitude of the magnetic field ( $B_{\text{max}}$  or  $B_{\text{min}}$ ) or the velocity of the solar wind as it passes over the magnetic poles of the planet,  $U_{\text{max}}$ , can also be easily understood from the dependence of the gyroradius on these quantities. As is well known (e.g., Jackson 1975), the gyroradius of a particle of charge  $q$  and mass  $m$ , in the presence of a uniform magnetic field of magnitude  $B$  and with a velocity perpendicular to the magnetic field  $V_{\perp}$ , is given by  $r_B = mcV_{\perp}/qB$ . A decrease in the magnetic field, or an increase in the characteristic velocity of the particle, results in an increment in  $r_B$  as found qualitatively in our results.

It is important to point out that additional complications in the magnetic field for the dayside ionosheath or in the density distribution of the newly born  $\text{O}^+$  ions, expected in a more realistic scenario than our simplified model, do not yield significant changes from the results presented. To analyze the effect of a different initial  $\text{O}^+$  ion distribution, with a maximum at the subsolar point, we have calculated the trajectory of  $\text{O}^+$  ions with a decreasing initial density distribution as a function of SZA. A SZA dependence of the density of newly born  $\text{O}^+$  ions may be expected as a result, for example, of a more efficient ionization process at the subsolar point, where solar wind ions are more abundant. We have chosen what may be considered an extreme scenario for such SZA dependence, by adopting a distribution decreasing exponentially by an order of magnitude from the subsolar point to the magnetic poles of the planet. Results for this case, which we label as Case 7, are shown in Figure 8, where we compare the average velocity components in a model with a uniform distribution in SZA (Case 1) with a case with the same

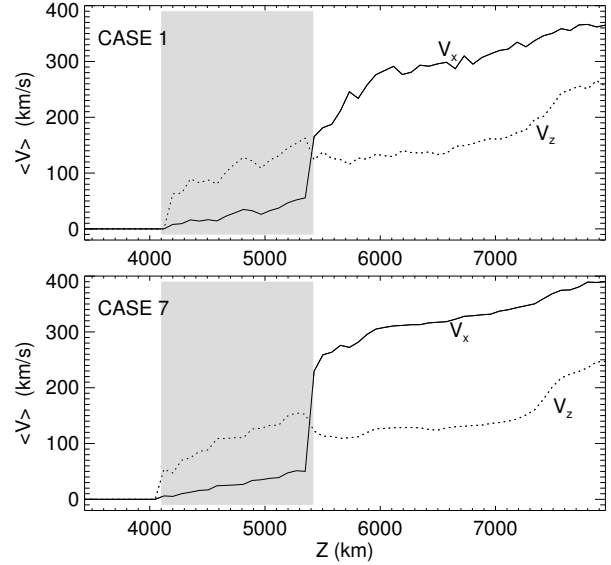


Fig. 8. Comparison of the vertical profiles of the average velocity of picked-up  $\text{O}^+$  ions over the magnetic poles of the planet, for different initial density distributions. The top panel corresponds to Case 1 already presented (see Table 1). The bottom panel corresponds to a model with the same parameters as Case 1 but with a density distribution exponentially decaying with SZA. The shaded region represents the height range travelled by the Mars Express spacecraft over the magnetic poles.

basic parameters ( $B_{\text{min}} = 10 \text{ nT}$ ,  $B_{\text{max}} = 60 \text{ nT}$  and  $U_{\text{max}} = 250 \text{ km s}^{-1}$ ) but with the exponential variation (in SZA) of the initial distribution of newly born  $\text{O}^+$  ions. We find that such an extreme increase of the abundance of  $\text{O}^+$  ions injected at low SZA affects mostly the average velocity at the “high” altitudes, where ions born near the subsolar point pass over the magnetic pole of the planet. However, below an altitude of approximately  $2000 \text{ km}$  over the magnetic poles of the planet, where the Mars Express spacecraft measurements described above were conducted, no significant change in the ratio of the  $\text{O}^+$  average velocity is observed.

We have also analysed the effect of a height dependent magnetic field intensity. If we adopt a magnetic field model in which the intensity depends also on the height above the ionopause, the gyroradius of a particle increases as it moves away from the planet, and its trajectory is even more “vertical” (in the positive  $z$  direction) as it passes over the magnetic pole. This is corroborated by calculations similar to those described in § 4, but not shown here for they do not change our main result. Hence, our conclusions remain unaltered by relaxing this simplifying assumption of our model.



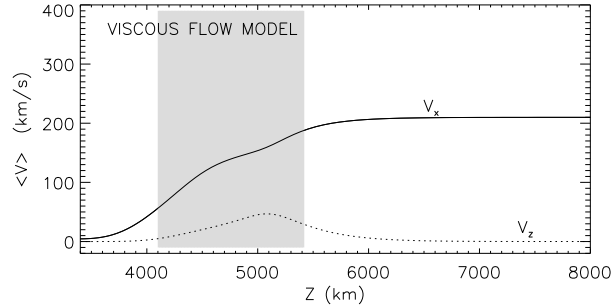


Fig. 9. Vertical profiles of the velocity of O<sup>+</sup> ions dragged by the solar wind over the magnetic poles of the planet in a viscous interaction model as described in the text. The thick solid line shows the  $x$  component of the velocity,  $V_x$ , and the dotted line shows  $V_z$ . The shaded region represents the height range travelled by the Mars Express spacecraft over the magnetic poles.

### 5.1. Prediction of the viscous flow model

In Reyes-Ruiz et al. (2008) we reported 2D hydrodynamic numerical simulations of the viscous interaction of the solar wind with the ionosphere of a non-magnetic planet in the vicinity of the magnetic poles of the planet. Such calculations have now been extended to follow the evolution of two distinct species, solar wind protons and ionospheric O<sup>+</sup> ions, to study the erosion of an ionosphere over the magnetic polar regions (Reyes-Ruiz & Pérez-de-Tejada 2008 and Reyes-Ruiz et al. 2009). These authors find that the properties of the flow in the ionosheath, over the magnetic polar regions, depend on the value of the effective Reynolds number (inversely proportional to the effective viscosity coefficient) and on the interspecies coupling timescale (in terms of the solar wind crossing timescale). Furthermore, they find that a Reynolds number of around 20 and an interspecies coupling timescale of the order of 0.1 are necessary to reproduce the location of the shock front and the intermediate transition (identified as the top of the viscous boundary layer) detected by *in situ* measurements in Venus and comets.

In Figure 9 we show the vertical profile of the velocity of O<sup>+</sup> ions in the vicinity of the magnetic poles of a non-magnetic planet according to the viscous flow model (Reyes-Ruiz et al. 2009). Results shown correspond to a fiducial case with Reynolds number equal to 20 and an interspecies coupling timescale of 0.1. The important feature of this result that we wish to point out is that in a viscous interaction model the ionospheric plasma over the magnetic poles is driven tailward, essentially in antisolar direction, by the transfer of momentum from the solar

wind. The horizontal ( $x$ ) component of the velocity greatly dominates over the vertical ( $z$ ) component. The ratio  $V_x/V_z$  has a typical value around 10, which is consistent with the ASPERA-3 measurements described previously (§ 3).

## 6. CONCLUSIONS

We have calculated the trajectory of O<sup>+</sup> ions born in the dayside ionosheath of Mars as they flow over the magnetic polar regions under the action of the advective electric field set up by the streaming solar wind and the IMF. By averaging the velocity of a large number of particles at a given height over the magnetic poles we determine the bulk velocity of O<sup>+</sup> ions. We find that for values of the magnetic field and solar wind velocity characteristic of the dayside ionosheath of Mars, the velocity over the magnetic poles is essentially vertical ( $z$ -direction) up to, at least, 2000 km in altitude. This result is in clear contradiction with *in situ* measurements taken with the ASPERA-3 instrument on board the Mars Express spacecraft, according to which the velocity of O<sup>+</sup> ions in such a region is strongly dominated by the  $x$  component. Hence, we conclude that, in the context of the magnetic field and solar wind velocity models considered here (which we consider represent correctly the conditions in the ionosheath) the gyromotion of O<sup>+</sup> ions alone can not explain the observed properties of the O<sup>+</sup> ion flow over the magnetic poles of the planet.

We emphasize that this conclusion is reached within the context of a restricted model for the geometry of the magnetic field and solar wind flow in the ionosheath. In future contributions we will consider the effect of the 3D character of the field and the solar wind flow in the ionosheath, as well as the importance of magnetic field fluctuations on the particle dynamics. Also, as more O<sup>+</sup> velocity data from the Mars Express mission, as well as from Venus Express, become publicly available, we plan to test if the conclusions we have reached are of a more general applicability than the single orbit results we have currently at our disposal.

Finally, in view of the consistency of the results of the viscous solar wind-ionosphere interaction models with the measurements of Mars Express, as discussed in the previous section, and the problems with the gyromotion interpretation, we consider that this measurement constitutes additional, indirect, evidence that viscous-like processes play an important role in the dynamics of the plasma environment of nonmagnetic planets.

MRR and HA acknowledge the financial support of DGAPA-Universidad Nacional Autónoma de México project IN109409-3.

## REFERENCES

- Acuña, M., et al. 1998, *Science*, 279, 1676  
 Barabash, S., et al. 2006, *Space Sci. Rev.*, 126, 113  
 Bertucci, C., et al. 2004, *AdSR*, 33, 1938  
 Bridge, H., Lazarus, A., Snyder, C., Smith, E., Davies, I., Coleman, P., & Jones, D. 1967, *Science*, 158, 1669  
 Crider, D. H., Brain, D. A., Acuña, M., Vignes, D., Mazelle, C., & Bertucci, C. 2004, *Space Sci. Rev.*, 111, 203  
 Jackson, J. D. 1975, *Classical Electrodynamics* (2nd ed.; New York: Wiley)  
 Lesieur, M. 1991, *Turbulence in Fluids* (Dordrecht: Kluwer)  
 Luhmann, J. G., & Schwingenshuh, K. 1990, *J. Geophys. Res.*, 95, 939  
 Lundin, R., Barabash, S., Fedorov, A., Holmström, M., Nilsson, H., Sauvaud, J.-A., & Yamauchi, M. 2008, *Geophys. Res. Lett.*, 35, 9203  
 Lundin, R., et al. 1990, *Geophys. Res. Lett.*, 17, 873  
 Lundin, R., et al. 2004, *Science*, 305, 1933  
 Pérez-de-Tejada, H. 1995, *Space Sci. Rev.*, 72, 655  
 \_\_\_\_\_ . 1998, *J. Geophys. Res.*, 103, 31499  
 \_\_\_\_\_ . 2001, *J. Geophys. Res.*, 106, 211  
 \_\_\_\_\_ . 2004, *AdSR*, 33, 167  
 \_\_\_\_\_ . 2005, *ApJ*, 618, L145  
 Pérez-de-Tejada, H., & Dryer, M. 1976, *J. Geophys. Res.*, 81, 2023  
 Pérez-de-Tejada, H., Intriligator, D. S., & Scarf, F. L. 1985, *J. Geophys. Res.*, 90, 1759  
 Pérez-de-Tejada, H., & Lundin, R. 2008, AGU Fall Meeting, Abstract P13B-1307  
 Pérez-de-Tejada, H., Lundin, R., Durand-Manterola, H., & Reyes-Ruiz, M. 2009, *J. Geophys. Res.*, 114, 106  
 Reyes-Ruiz, M., Díaz-Méndez, E., & Pérez-de-Tejada, H. 2008, *A&A*, 489, 1319  
 Reyes-Ruiz, M., & Pérez-de-Tejada, H. 2008, AGU Fall Meeting, Abstract P13B-1313  
 Reyes-Ruiz, M., Pérez-de-Tejada, H., Aceves, H., & Vázquez, R. 2009, arXiv:0812.1189  
 Riedler, W., et al. 1991, *Planet. Space Sci.*, 39, 75  
 Romanov, S. A., Smirnov, V., & Vaisberg, O. 1979, *Cosmic Res.*, 16, 603  
 Shefer, R., Lazarus, A., & Bridge, H. 1979, *J. Geophys. Res.*, 84, 2109  
 Spreiter, J., & Stahara, S. 1980, *J. Geophys. Res.*, 85, 7715

Mauricio Reyes-Ruiz and Héctor Aceves: Instituto de Astronomía, Universidad Nacional Autónoma de México, Apdo. Postal 877, 22800 Ensenada, B. C., Mexico (maurey@astro.unam.mx, aceves@astro.unam.mx).  
 Héctor Pérez-de-Tejada: Instituto de Geofísica, Universidad Nacional Autónoma de México, 04510 Mexico D.F., Mexico (Pérezdet@geofisica.unam.mx).